Optimal Spectral Decomposition (OSD) for GTSPP Data Analysis

Peter C Chu[1],Charles Sun[2], & Chenwu Fan[1]

[1] Naval Postgraduate School, Monterey, CA 93943

pcchu@nps.edu, http://faculty.nps.edu/pcchu/

[2] NOAA/NODC, Silver Spring, MD 20910

Charles.Sun@noaa.gov

GTSPP Meeting, Oostende, Belgium, 5-7 May 2010.

Observational Data

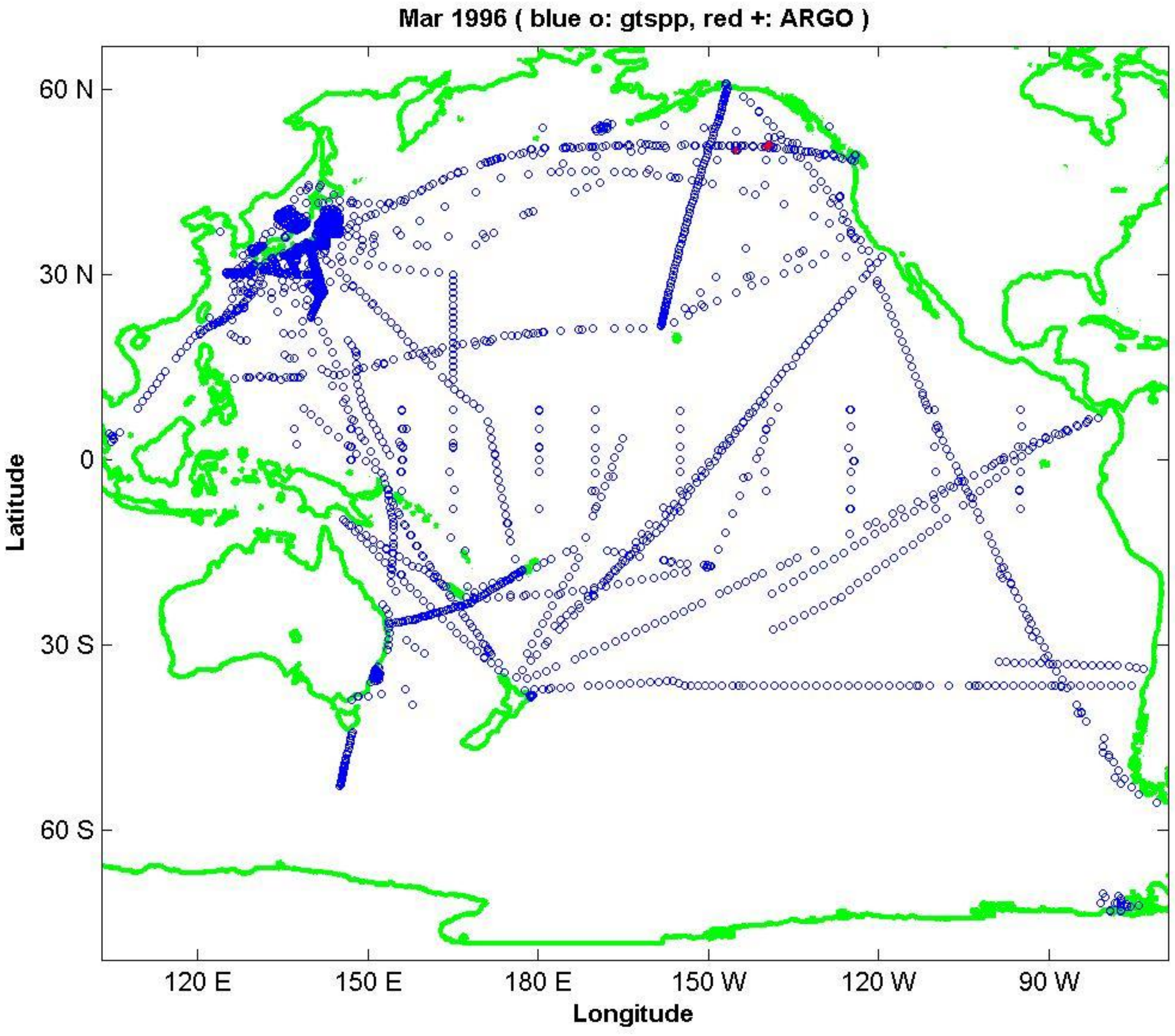

It is an urgent need to establish monthly varying (T, S, u, v) gridded dataset from GTSPP and Argo trajectory data →

Oceanographic and Climate Studies

Ocean Data Analysis

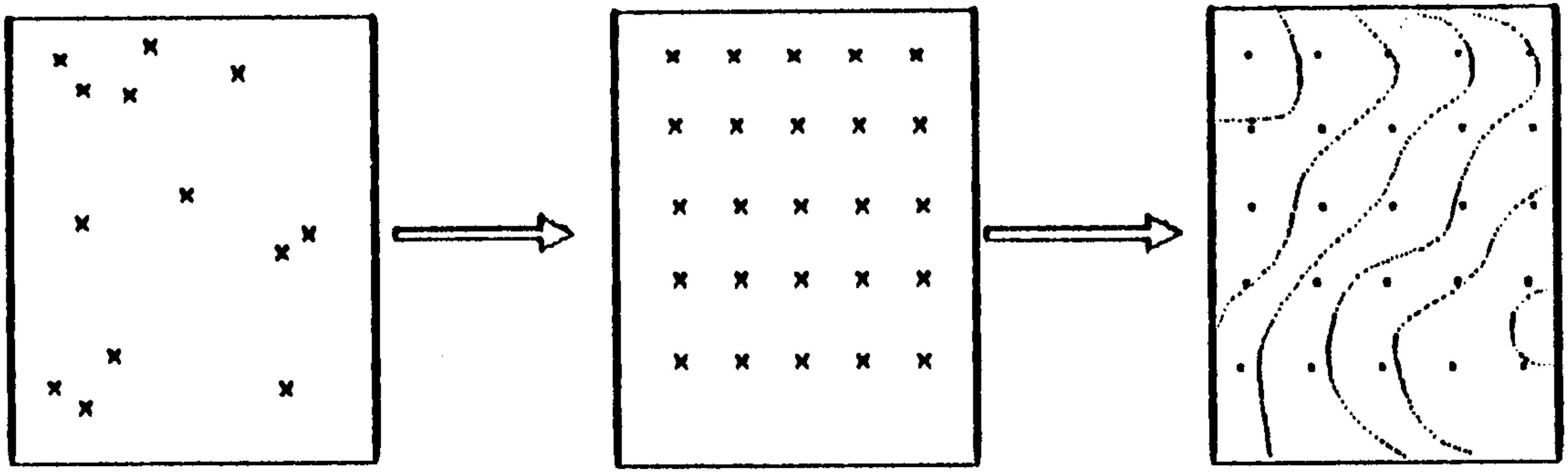

Classical Method → Fourier Series Expansion

Joseph Fourier 1768-1830

Fourier was obsessed with the physics of heat and developed the Fourier series and transform to model heat-flow problems.

Fourier Series Expansion

For a rectangular region (L_x, L_y), the basis functions are sinusoidal functions.

$$f(x,y) = \sum_i \sum_j a_{ij} \sin\frac{i\pi x}{L_x} \sin\frac{j\pi y}{L_y}$$

$$+\sum_i \sum_j b_{ij} \cos\frac{i\pi x}{L_x} \cos\frac{j\pi y}{L_y}$$

For the Dirichret boundary condition : $f = 0$ at the boundaries

$$f(x,y) = \sum_i \sum_j a_{ij} \sin\frac{i\pi x}{L_x} \sin\frac{j\pi y}{L_y}$$

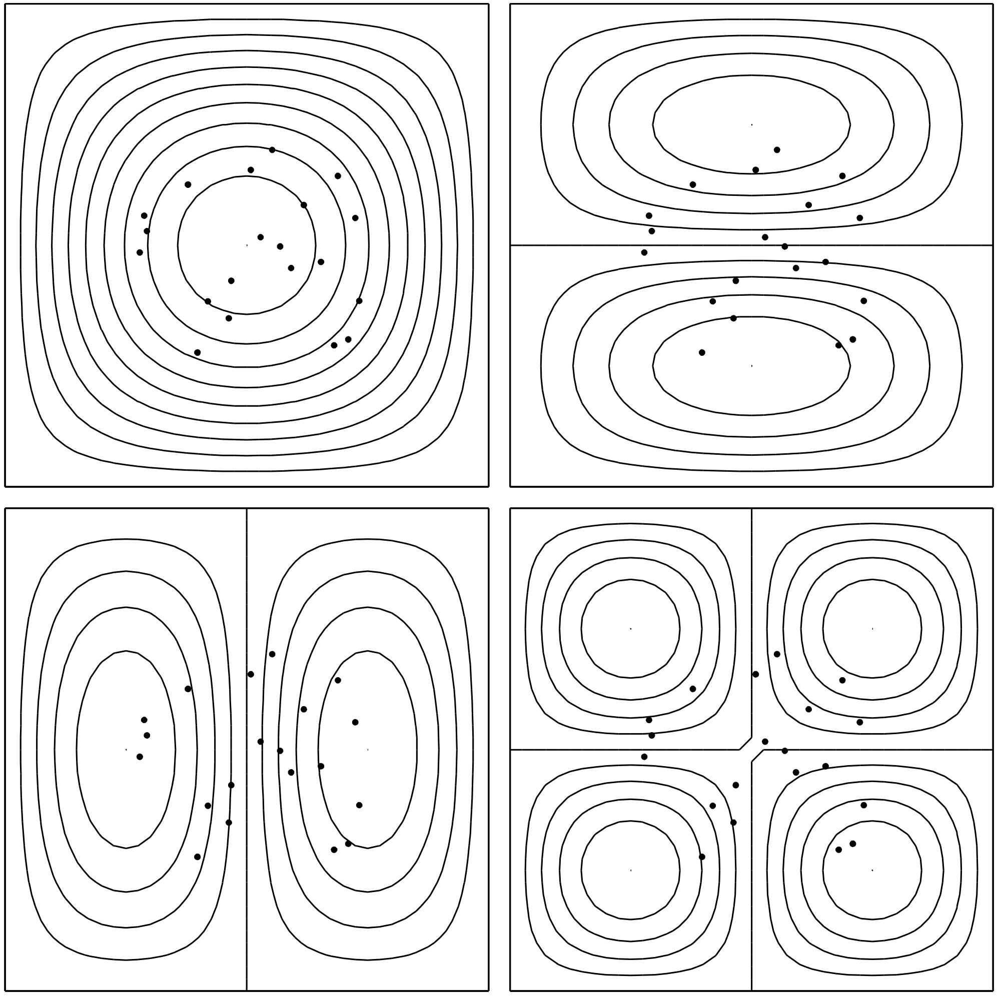

The dots represent the Observations.

Linear Algebraic Equations for the Coefficients a_{ij}

$$f(x_1^{ob}, y_1^{ob}) = \sum_i \sum_j a_{ij} \sin\frac{i\pi x_1^{ob}}{L_x} \sin\frac{j\pi y_1^{ob}}{L_y}$$

$$f(x_2^{ob}, y_2^{ob}) = \sum_i \sum_j a_{ij} \sin\frac{i\pi x_2^{ob}}{L_x} \sin\frac{j\pi y_2^{ob}}{L_y}$$

……

$$f(x_M^{ob}, y_M^{ob}) = \sum_i \sum_j a_{ij} \sin\frac{i\pi x_M^{ob}}{L_x} \sin\frac{j\pi y_M^{ob}}{L_y}$$

Determination of Spectral Coefficients (Ill-Posed Algebraic Equation)

$$\mathbf{A}\hat{\mathbf{a}} = \mathbf{Q}\mathbf{Y},$$

Known a_{ij} → Analyzed Field

$$f(x,y)=\sum_i \sum_j a_{ij} \sin\frac{i\pi x}{L_x} \sin\frac{j\pi y}{L_y}$$

For the Neumann boundary condition $n \bullet \nabla f = 0$
at the boundaries

$$f(x,y) = \sum_i \sum_j b_{ij} \cos\frac{i\pi x}{L_x} \cos\frac{j\pi y}{L_y}$$

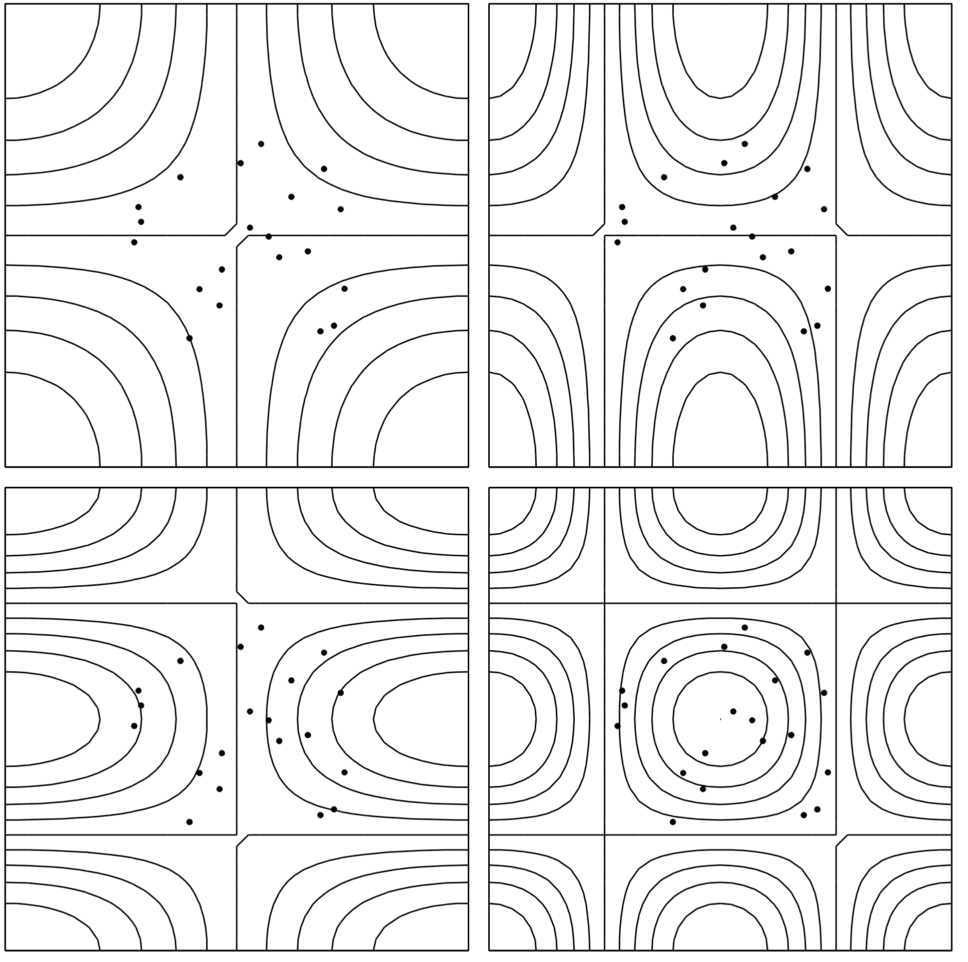

The dots represent the Observations.

Linear Algebraic Equations for the Coefficients a_{ij}

$$f(x_1^{ob}, y_1^{ob}) = \sum_i \sum_j b_{ij} \cos\frac{i\pi x_1^{ob}}{L_x} \cos\frac{j\pi y_1^{ob}}{L_y}$$

$$f(x_2^{ob}, y_2^{ob}) = \sum_i \sum_j b_{ij} \cos\frac{i\pi x_2^{ob}}{L_x} \cos\frac{j\pi y_2^{ob}}{L_y}$$

……

$$f(x_M^{ob}, y_M^{ob}) = \sum_i \sum_j b_{ij} \cos\frac{i\pi x_M^{ob}}{L_x} \cos\frac{j\pi y_M^{ob}}{L_y}$$

Known b_{ij} → Analyzed Field

$$f(x,y)=\sum_i\sum_j b_{ij}\cos\frac{i\pi x}{L_x}\cos\frac{j\pi y}{L_y}$$

For General Ocean Basin → Generalized Fourier Series Expansion

Spectral Representation
Fourier Series Expansion

$$c(\mathbf{x}, z_k, t) = A_0(z_k, t) + \sum_{m=1}^{M} A_m(z_k, t)\ \Psi_m(\mathbf{x}, z_k),$$

Ψ_m → Basis functions (not sinusoidal)

c → any ocean variable

Determination of Basis Functions

- (1) Eigen Functions of the Laplace Operator (Data and Model Independent)
- (2) Empirical Orthogonal Functions (Data or Model Dependent)

Eigen Functions of Laplace Operator → Basis Functions (Closed Basin)

$$\Delta\Psi_k = -\lambda_k \Psi_k, \quad \Psi_k|_\Gamma = 0, \qquad k = 1, ..., \infty$$

$$\Delta\Phi_m = -\mu_m \Phi_m, \quad \frac{\partial \Phi_m}{\partial n}|_\Gamma = 0, \qquad m = 1, ..., \infty.$$

Ψ_k → Streamfunction

Φ_m → T, S, Velocity Potential

Basis Functions (Open Boundaries)

$$\triangle \Psi_k = -\lambda_k \Psi_k,$$

$$\triangle \Phi_m = -\mu_m \Phi_m,$$

$$\Psi_k|_\Gamma = 0, \quad \frac{\partial \Phi_m}{\partial n}|_\Gamma = 0,$$

$$\left[\frac{\partial \Psi_k}{\partial n} + \kappa(\tau)\Psi_k\right]|_{\Gamma_1'} = 0, \quad \Phi_m|_{\Gamma_1'} = 0,$$

Boundary Conditions

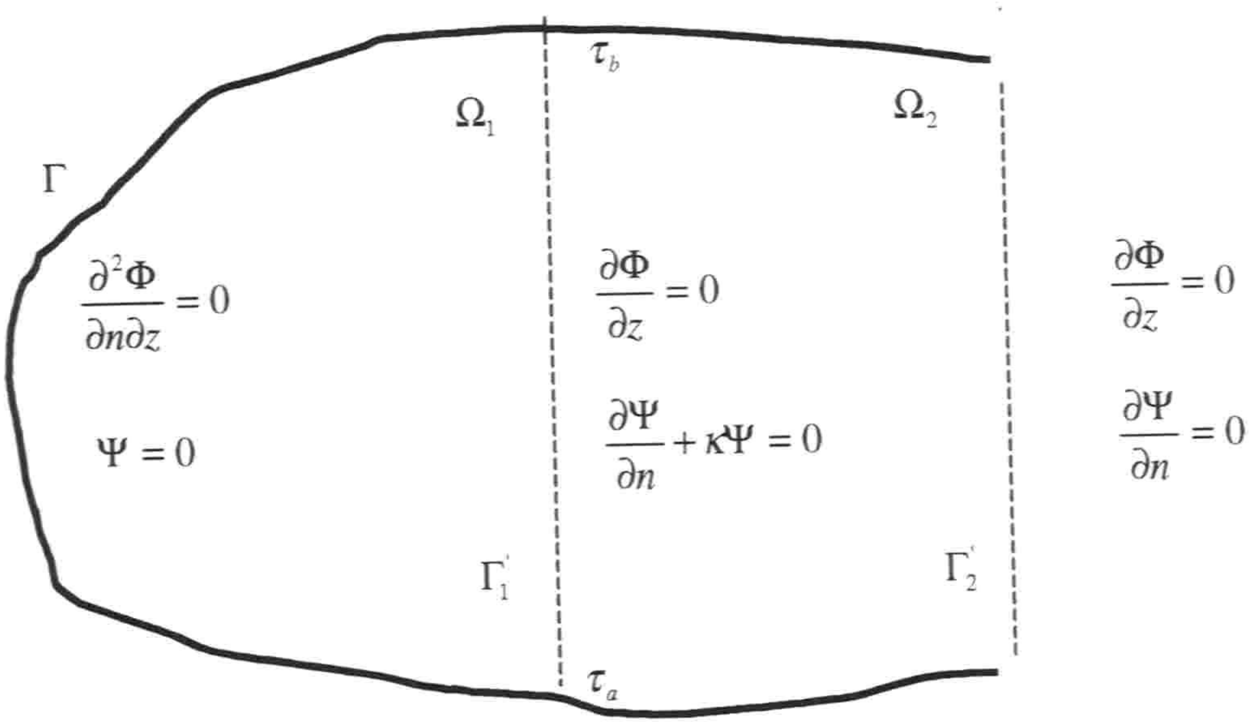

Spectral Decomposition

$$u_{KM} = \sum_{k=1}^{K} a_k(z, t^\circ) \frac{\partial \Psi_k(x, y, z, \kappa^\circ)}{\partial y} + \sum_{m=1}^{M} b_m(z, t^\circ) \frac{\partial \Phi_m(x, y, z)}{\partial x},$$

$$v_{KM} = -\sum_{k=1}^{K} a_k(z, t^\circ) \frac{\partial \Psi_k(x, y, z, \kappa^\circ)}{\partial x} + \sum_{m=1}^{M} b_m(z, t^\circ) \frac{\partial \Phi_m(x, y, z)}{\partial y}$$

$$T(\mathbf{x}, t) = T_0(\mathbf{x}) + \sum_{m=1}^{M} c_m(t) \Phi_m(\mathbf{x})$$

$$S(\mathbf{x}, t) = S_0(\mathbf{x}) + \sum_{m=1}^{M} d_m(t) \Phi_m(\mathbf{x})$$

Benefits of Using OSD

- (1) Don’t need first guess field
- (2) Don’t need autocorrelation functions
- (3) Don’t require high signal-to-noise ratio
- (4) Basis functions are pre-determined before the data analysis. They are independent on the data.

Optimal Mode Truncation

$$J(a_{1,\ldots,}a_K, b_{1,\ldots,}b_M, \kappa, P) = \frac{1}{2}\left(\left\|u_p^{obs} - u_{KM}\right\|_P^2 + \left\|v_p^{obs} - v_{KM}\right\|_P^2\right) \rightarrow \min,$$

Vapnik (1983) Cost Function

$$J_{emp} = J(a_{1,\ldots,}a_{K,}b_{1,\ldots,}b_M, \kappa, P).$$

$$\mathrm{Prob}\left\{\sup_{K,M,S} |\langle J(K,M,S)\rangle - J_{emp}(K,M,S)| \geq \mu\right\} \leq g(P,\mu)$$

$$\lim_{P\to\infty} g(P,\mu) = 0$$

Optimal Truncation

- Gulf of Mexico, Monterey Bay, Louisiana-Texas Shelf, North Atlantic
- $K_{opt} = 40$, $M_{opt} = 30$

Determination of Spectral Coefficients (Ill-Posed Algebraic Equation)

$$\mathbf{A}\hat{\mathbf{a}} = \mathbf{Q}\mathbf{Y},$$

This is caused by the features of the matrix **A**.

Rotation Method (Chu et al., 2004)

Well-Posed → $$\mathbf{S}\mathbf{A}\hat{\mathbf{a}} = \mathbf{S}\mathbf{Q}\mathbf{Y},$$

The matrix S is determined by

$$J_1 = \|\mathbf{A}\|^2 - \frac{\|\mathbf{SQY}\|^2}{\|\mathbf{a}\|^2} \rightarrow \max,$$

Errors

$$\bar{T}(\mathbf{x}) = \overbrace{T_0 + \sum_{l=1}^{48} D_l \Phi_l(\mathbf{x})}^{\hat{T}} + T'(\mathbf{x})$$

$$\bar{\mathbf{u}}(\mathbf{x}, t) = \overbrace{C\Psi_0 + \sum_{n=1}^{24} A_n \nabla \times \mathbf{k}\Psi_n(\mathbf{x})}^{\hat{\mathbf{u}}} + \tilde{\mathbf{u}}(\mathbf{x}) + \mathbf{u}'(\mathbf{x})$$

T’ , **u**’ → errors

Noise-to-Signal Ratio → Error Estimation

$$\eta\left(\boldsymbol{\alpha},\boldsymbol{\beta}\right)=\frac{\left\|\boldsymbol{\alpha}\right\|_{(P)}}{\left\|\boldsymbol{\beta}\right\|_{(P)}}$$

$$\eta(T',T-T') \sim 0.1$$

OSD Applications

(a) Baroclinic Rossby Waves in the tropical North Atlantic at mid-depth (Argo Trajectory Data)

(b) Synoptic Current Reversals on the Texas-Louisiana Continental Shelf (Surface Drifting Buoys)

(c) Monterey Bay Surface Circulation (CODAR)

(d) Synoptic (T, S) Fields for Pacific

(a) Baroclinic Rossby Waves in the tropical North Atlantic at mid-depth (ARGO)

References

- Chu, P.C., L.M. Ivanov, and O.M. Melnichenko, 2005: Fall-winter current reversals on the Texas-Lousiana continental shelf. Journal of Physical Oceanography, 35, 902-910

- Chu, P.C., L.M. Ivanov, O.M. Melnichenko, and N.C. Wells, 2007: On long baroclinic Rossby Waves in the tropical North Atlantic observed from profiling floats. Journal of Geophysical Research – Oceans, 112, C05032, doi:10.1029/2006JC003698.

- These papers can be downloaded from:
- http://www.nps.edu/pcchu

Tropical North Atlantic (4º -24ºN) Important Transition Zone → Meridional Overturning Circulation (MOC)

(Rahmstorf 2006)

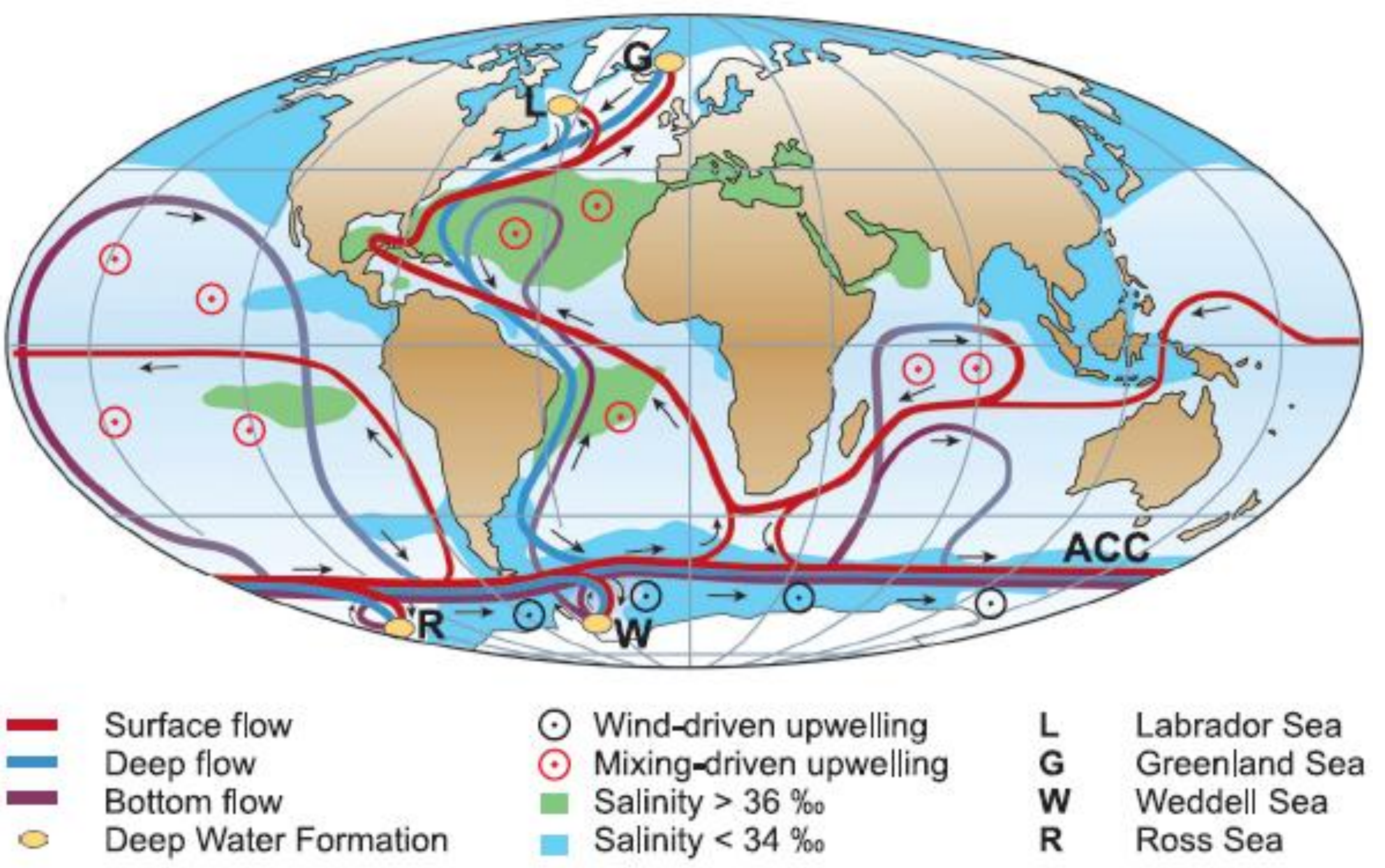

MOC Variation →

Heat Transport Variation →

Climate Change

- Are mid-depth (~1000 m) ocean circulations steady?

- If not, what mechanisms cause the change? (Rossby wave propagation)

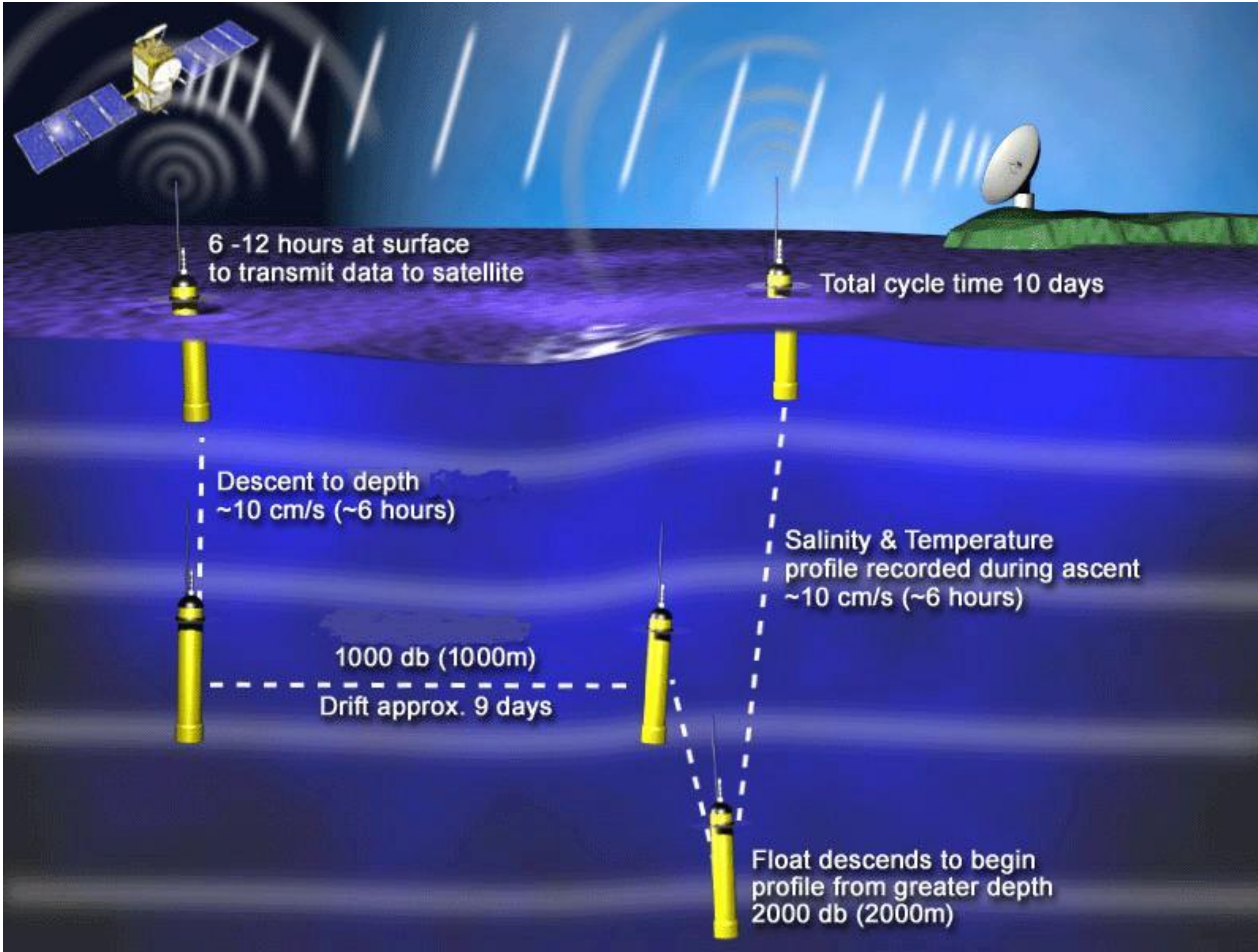
6 -12 hours at surface
to transmit data to satellite
Total cycle time 10 days
Descent to depth
~10 cm/s (~6 hours)
Salinity & Temperature
profile recorded during ascent
~10 cm/s (~6 hours)
1000 db (1000m)
Drift approx. 9 days
Float descends to begin
profile from greater depth
2000 db (2000m)

Argo Observations (Oct-Nov 2004)

(a) Subsurface tracks

(b) Float positions where (T,S) were measured

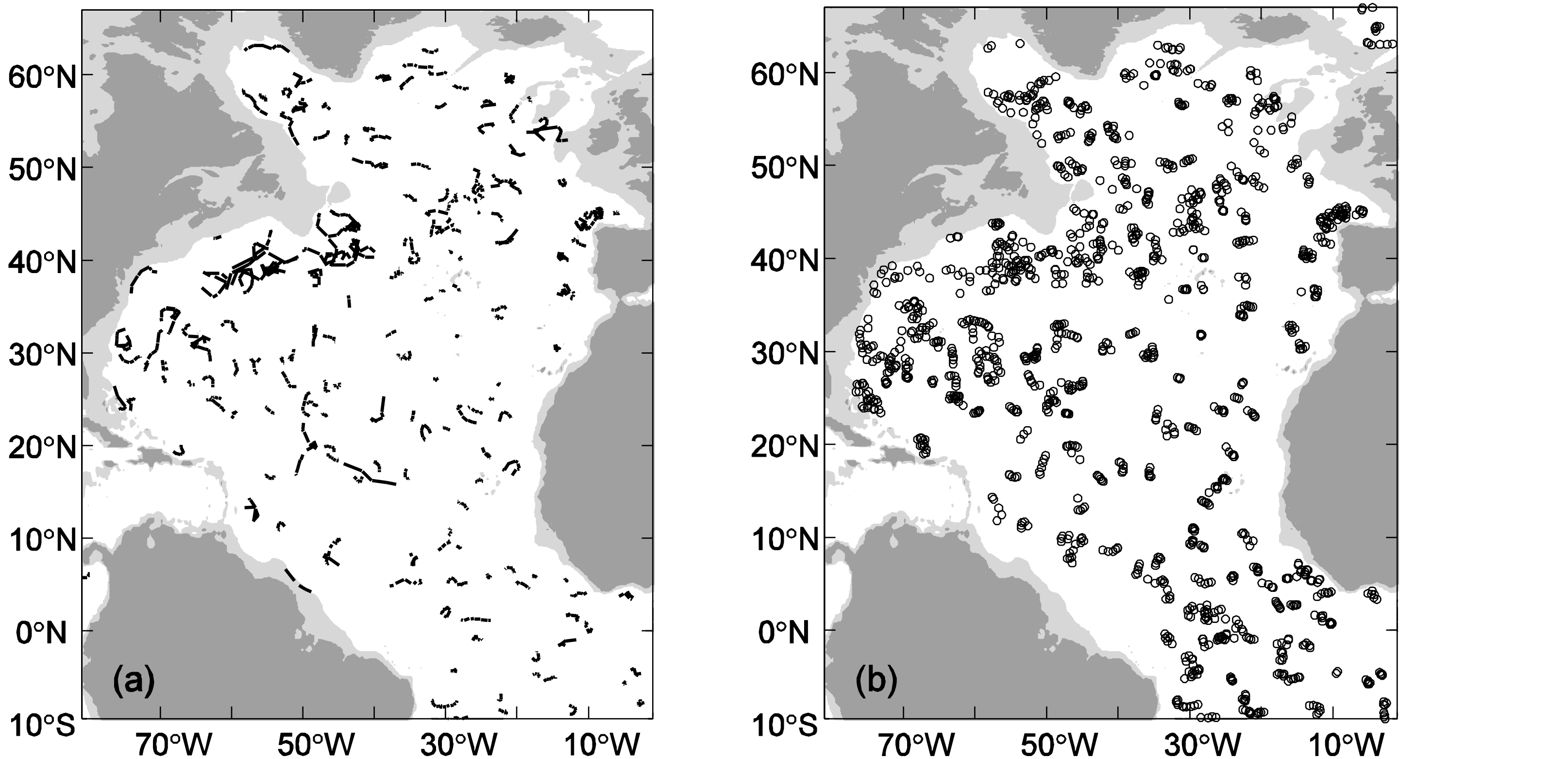

Circulations at 1000 m estimated from the original ARGO float tracks (bin method)
April 2004 – April 2005

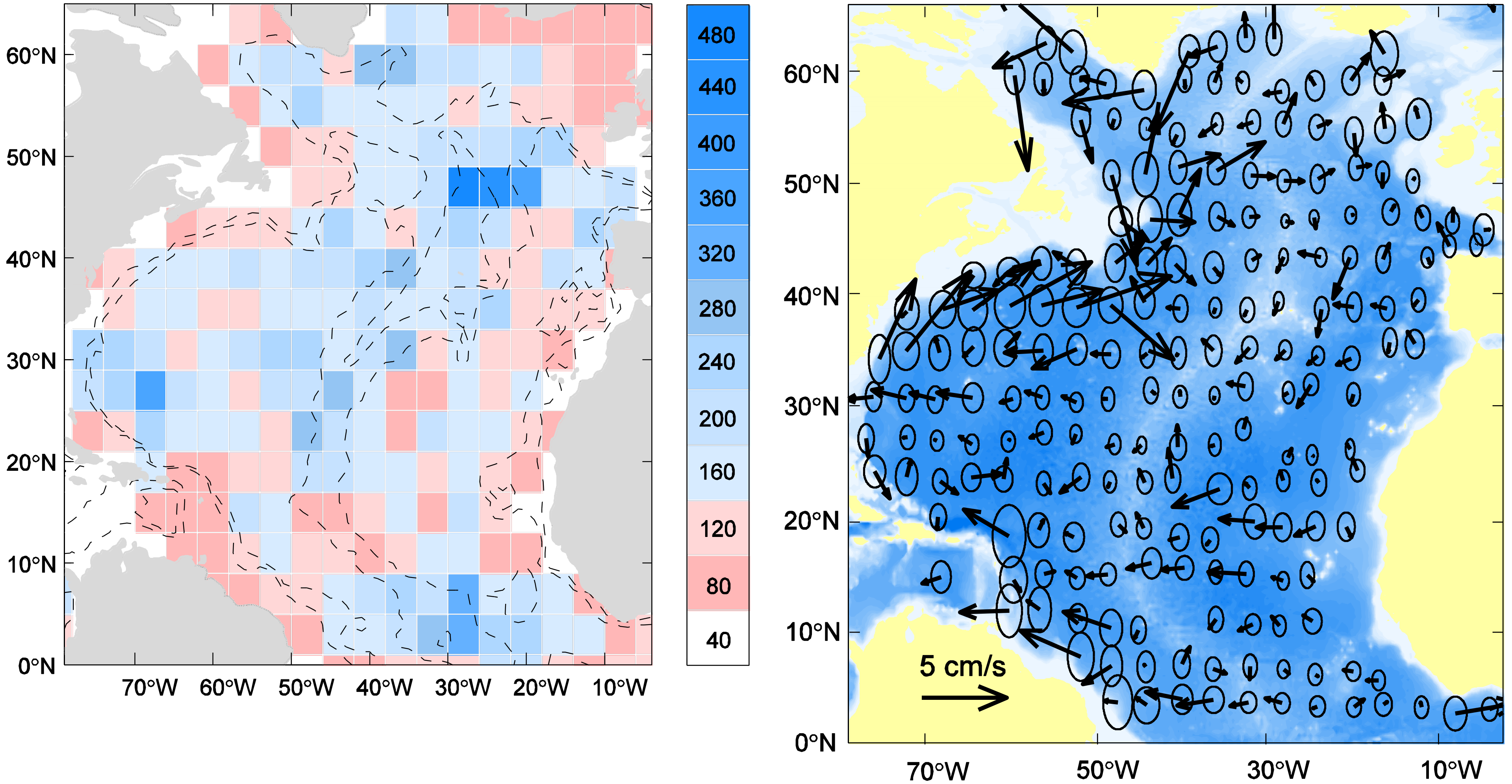

It is difficult to use such noisy data into ocean numerical models.

Boundary Configuration → Basis Functions for OSD

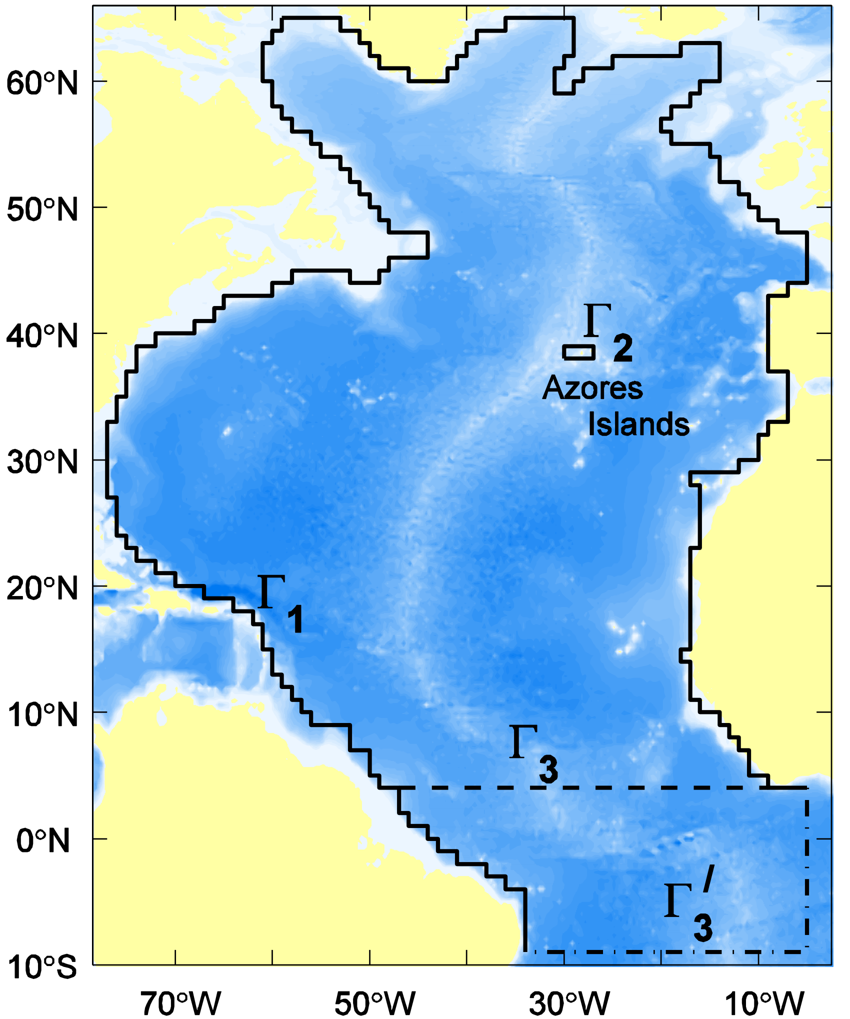

Basis Functions for Streamfunction Mode-1 and Mode-2

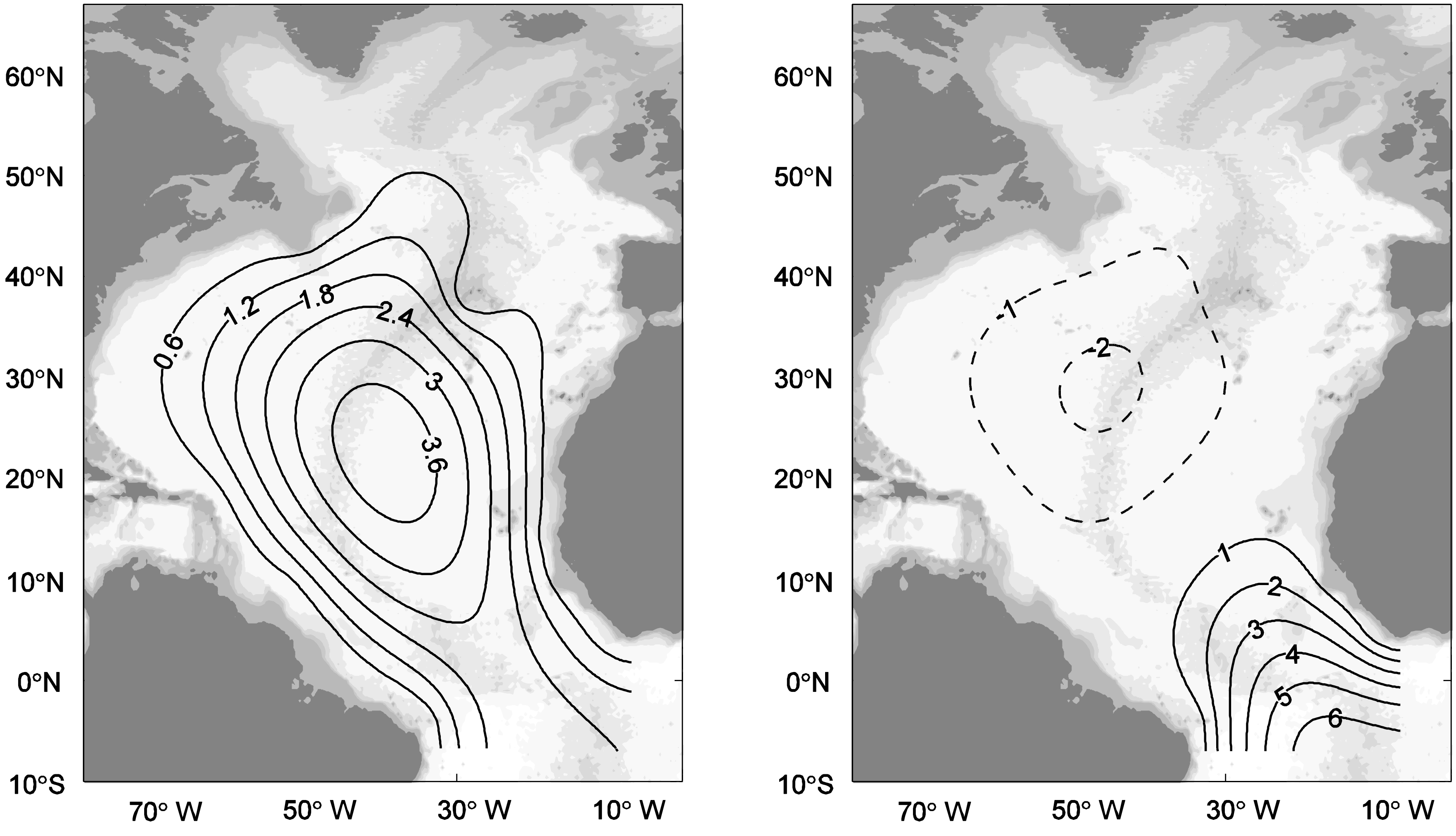

Circulations at 1000 m (March 04 to May 05)

Bin Method

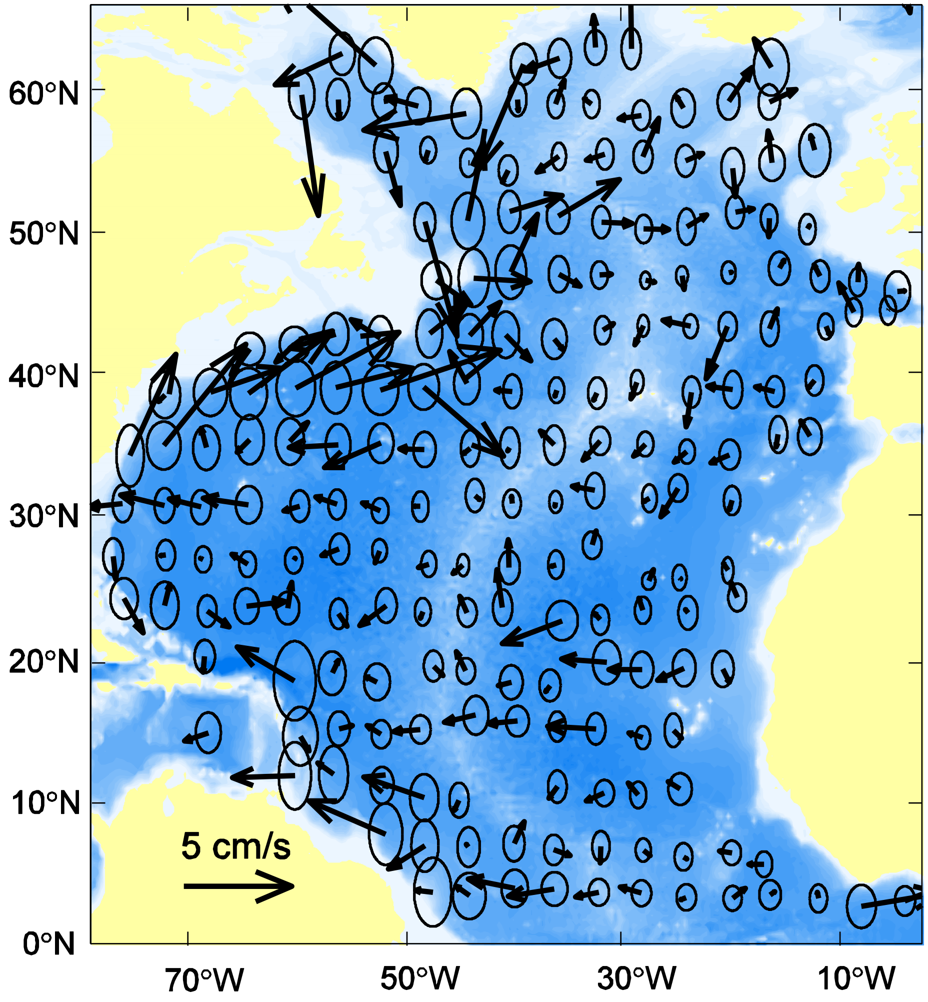

OSD

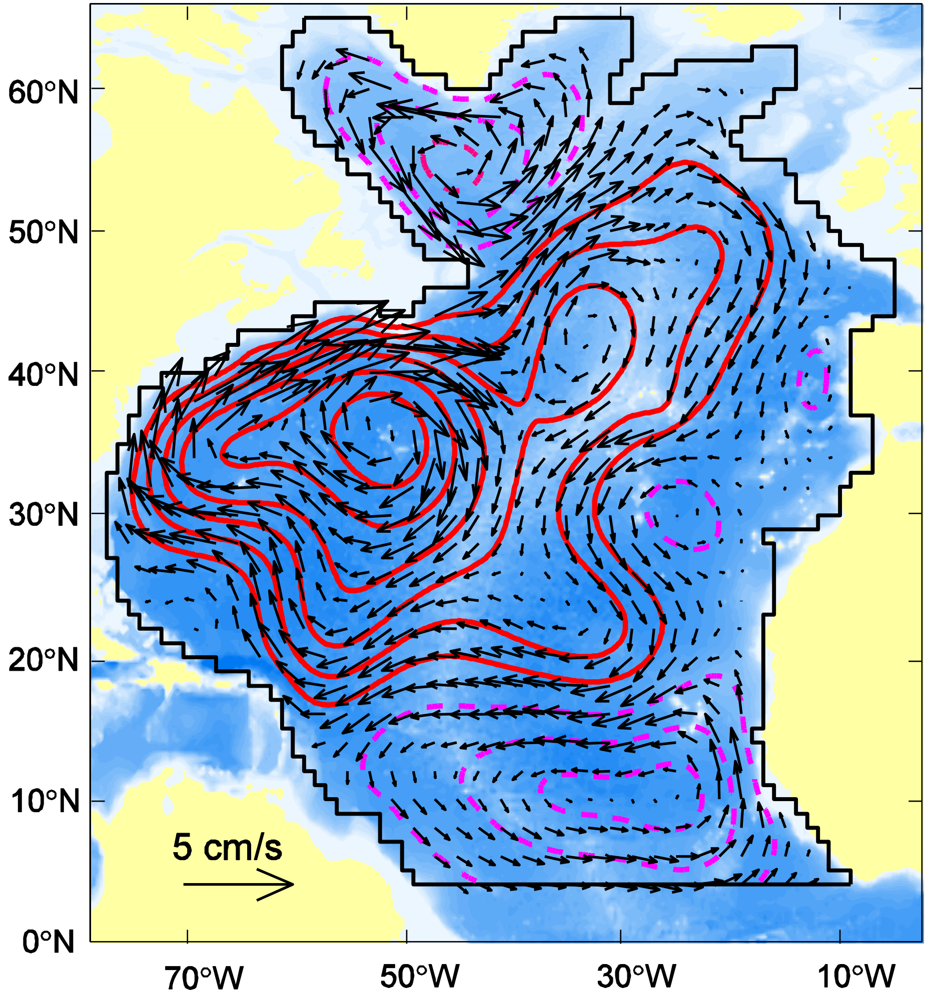

Fourier Expansion → Temporal Annual and Semi-anuual

$$\hat{\psi} \approx \overline{\psi}(\mathbf{x}_\perp) + \psi_1(\mathbf{x}_\perp, t) + \psi_2(\mathbf{x}_\perp, t),$$

$$\psi_1(\mathbf{x}_\perp, t) = \sum_{s=1}^{2} A_{\omega_1,s} \cos(\omega_1 t + \theta_{\omega_1,s}) Z_s(\mathbf{x}_\perp) + \sum_{k=1}^{K_{opt}} B_{\omega_1,k} \cos(\omega_1 t + \vartheta_{\omega_1,k}) \Psi_k(\mathbf{x}_\perp),$$

$$\psi_2(\mathbf{x}_\perp, t) = \sum_{s=1}^{2} A_{\omega_2,s} \cos(\omega_2 t + \theta_{\omega_2,s}) Z_s(\mathbf{x}_\perp) + \sum_{k=1}^{K_{opt}} B_{\omega_2,k} \cos(\omega_2 t + \vartheta_{\omega_2,k}) \Psi_k(\mathbf{x}_\perp),$$

T_0=12 months; $\omega_1 = 2\pi / T_0$; $\omega_2 = 4\pi / T_0$

Fourier Expansion → Temporal Annual and Semi-anuual

$$\hat{T}(\mathbf{x}_\perp, z, t) \approx \overline{T}(\mathbf{x}_\perp, z) + T_1(\mathbf{x}_\perp, z, t) + T_2(\mathbf{x}_\perp, z, t),$$

$$T_1(\mathbf{x}_{\perp,} z, t) = \sum_{m=1}^{M_{opt}} C_{\omega_1, m}(z) \cos[\omega_1 t + \chi_{\omega_1, m}(z)] \Xi_m(\mathbf{x}_\perp, z),$$

$$T_2(\mathbf{x}_{\perp,} z, t) = \sum_{m=1}^{M_{opt}} C_{\omega_2, m}(z) \cos[\omega_2 t + \chi_{\omega_{21}, m}(z)] \Xi_m(\mathbf{x}_\perp, z),$$

T_0=12 months; $\omega_1 = 2\pi / T_0$; $\omega_2 = 4\pi / T_0$

Optimization

$$J_s = \int_{t_o}^{t_o+T_o} \left[a_s(t) - \sum_{\omega=\omega_1,\omega_2} A_{\omega,s} \cos(\omega t + \theta_{\omega,s}) \right]^2 dt \to \min$$

$$I_k = \int_{t_o}^{t_o+T_o} \left[b_k(t) - \sum_{\omega=\omega_1,\omega_2} B_{\omega,s} \cos(\omega t + \vartheta_{\omega,s}) \right]^2 dt \to \min$$

Annual Component

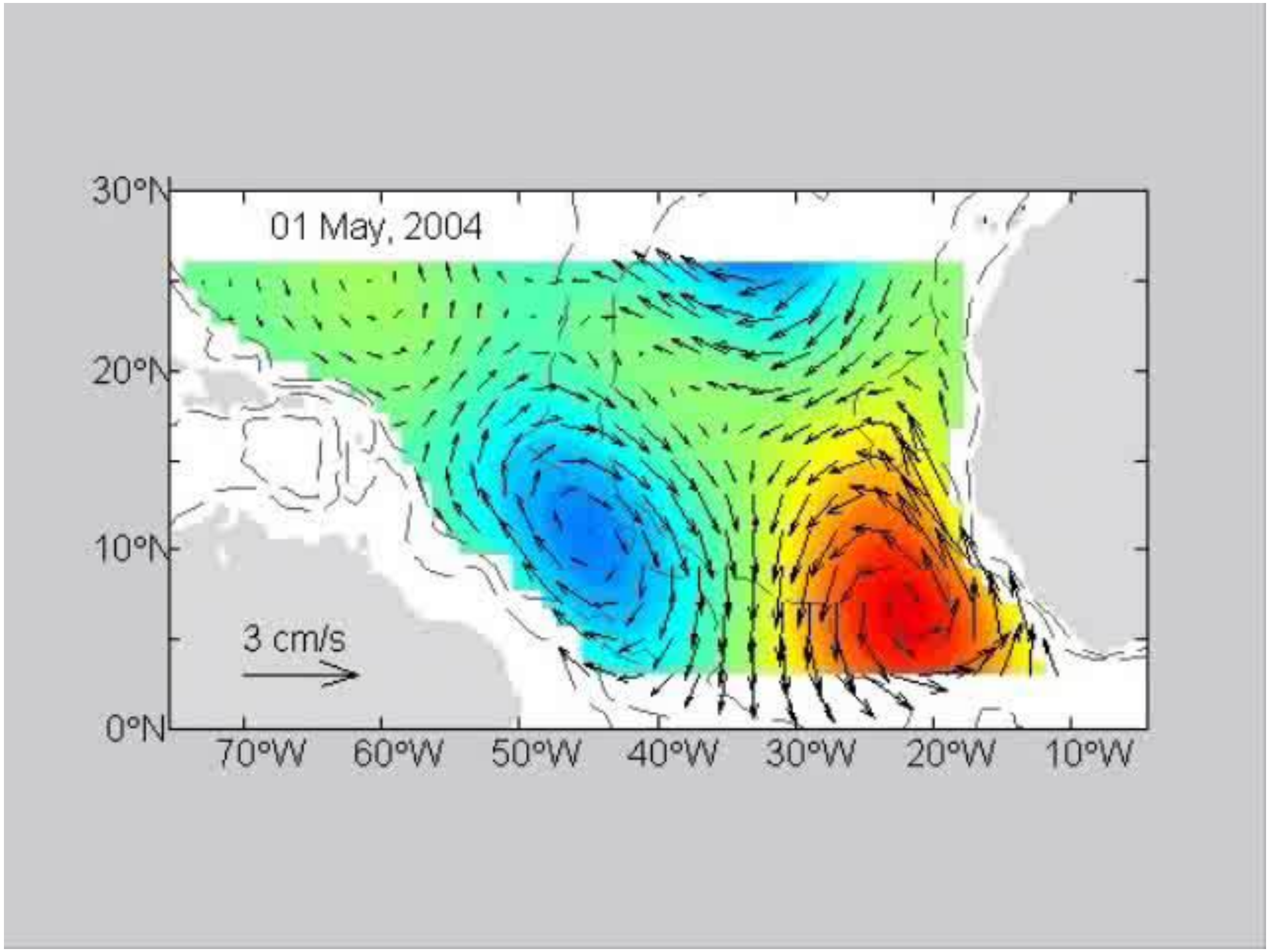

Semi-annual Component

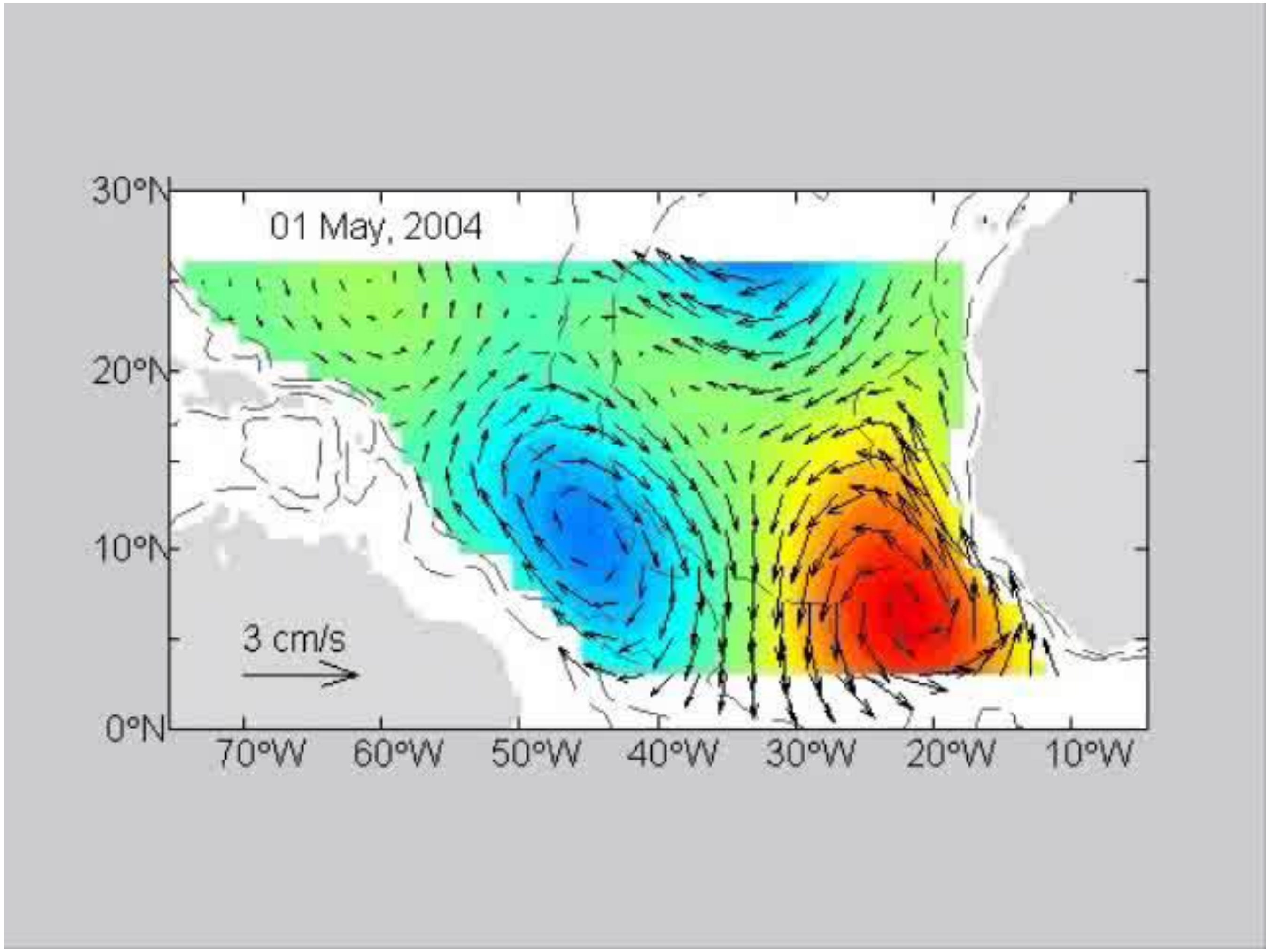

Time –Longitude Diagrams of Meridional Velocity Along 11ºN

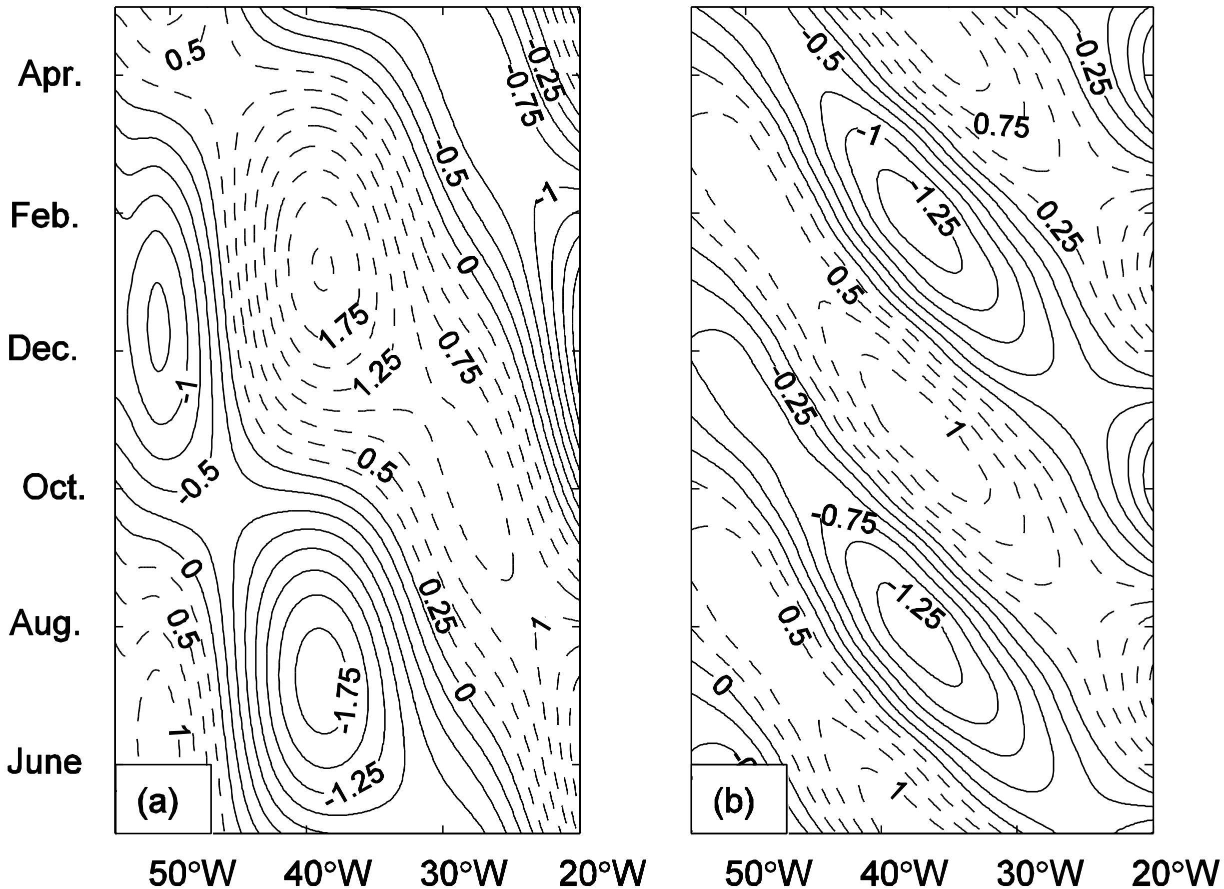

Annual

Semi-Annual

Time –Longitude Diagrams of temperature Along 11ºN

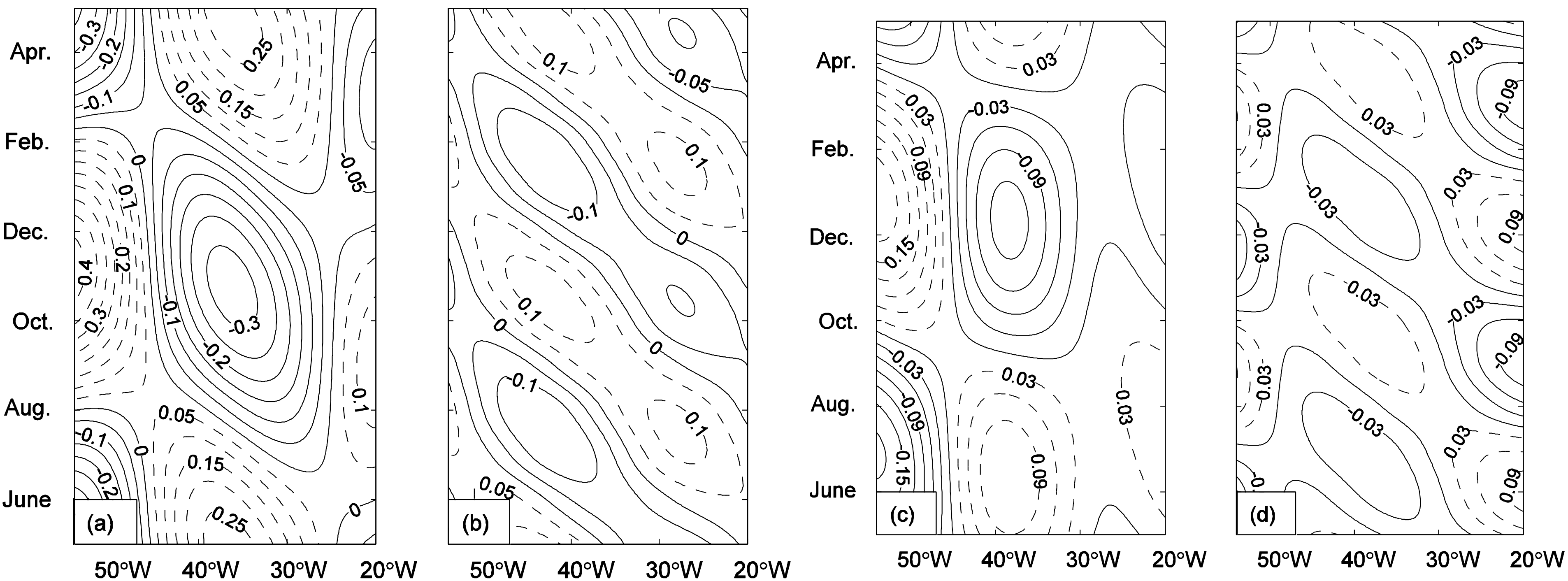

Annual

Semi-Annual

Annual

Semi-Annual

550 m

950 m

Characteristics of Annual Rossby Waves

	March, 04 – May, 05 float data			March, 04 – May, 06 float data		
Latitude	c_p (cm/s)	L_1 (km)	L_2 (km)	c_p (cm/s)	L_1 (km)	L_2 (km)
5^0N	12	1200	1100	12	1300	900
8^0N	16	2500	1400	12	2100	1100
11^0N	14	2200	1400	11	1900	1100
13^0N	11	2100	1500	10	2300	1500

Western Basin　Eastern Basin　Western Basin　Eastern Basin

(b) Synoptic Current Reversals on the Texas-Louisiana Continental Shelf (Surface Drifting Buoys)

Ocean Velocity Observation

- 31 near-surface (10-14 m) current meter moorings during LATEX from April 1992 to November 1994
- Drifting buoys deployed at the first segment of the Surface Current and Lagrangian-drift Program (SCULP-I) from October 1993 to July 1994.

Moorings and Buoys

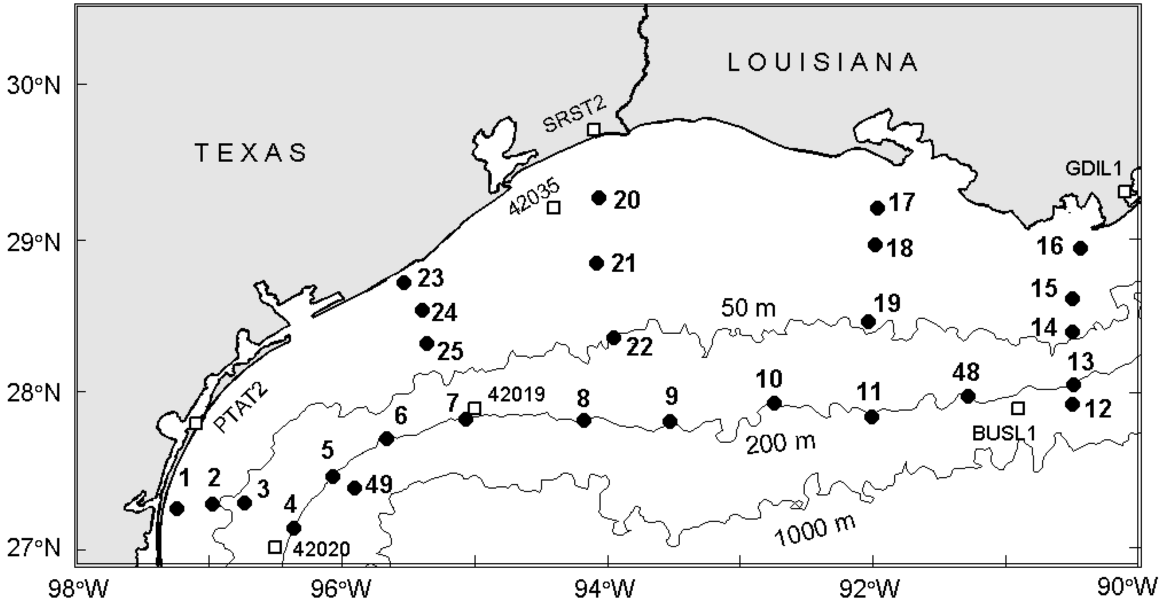

LTCS current reversal detected from SCULP-I drift trajectories.

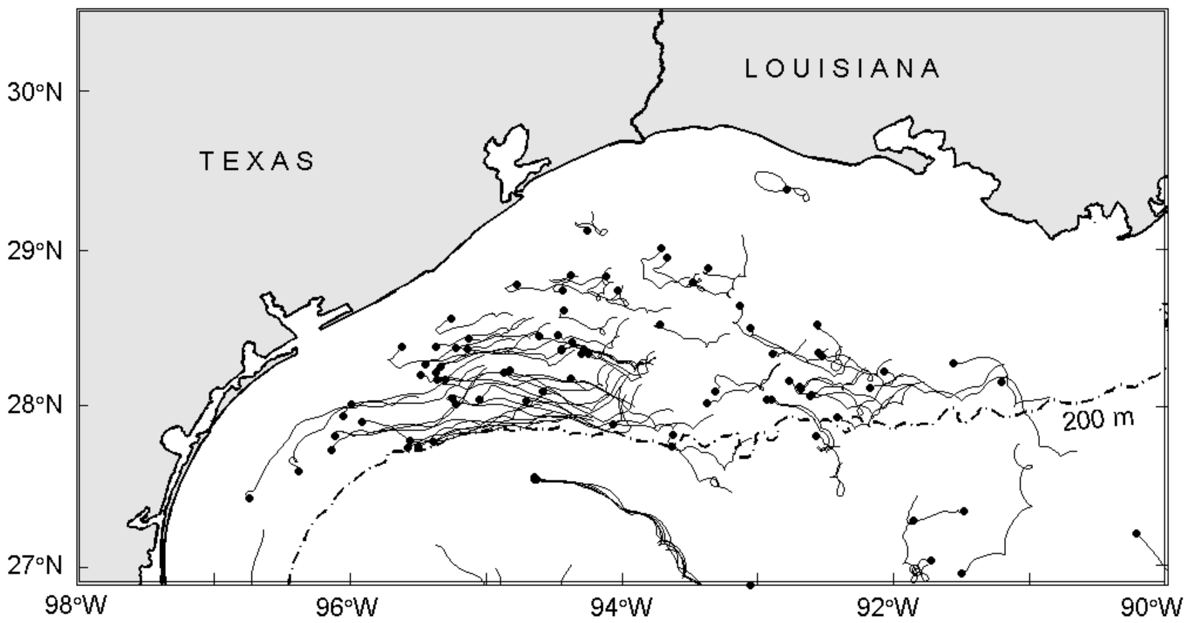

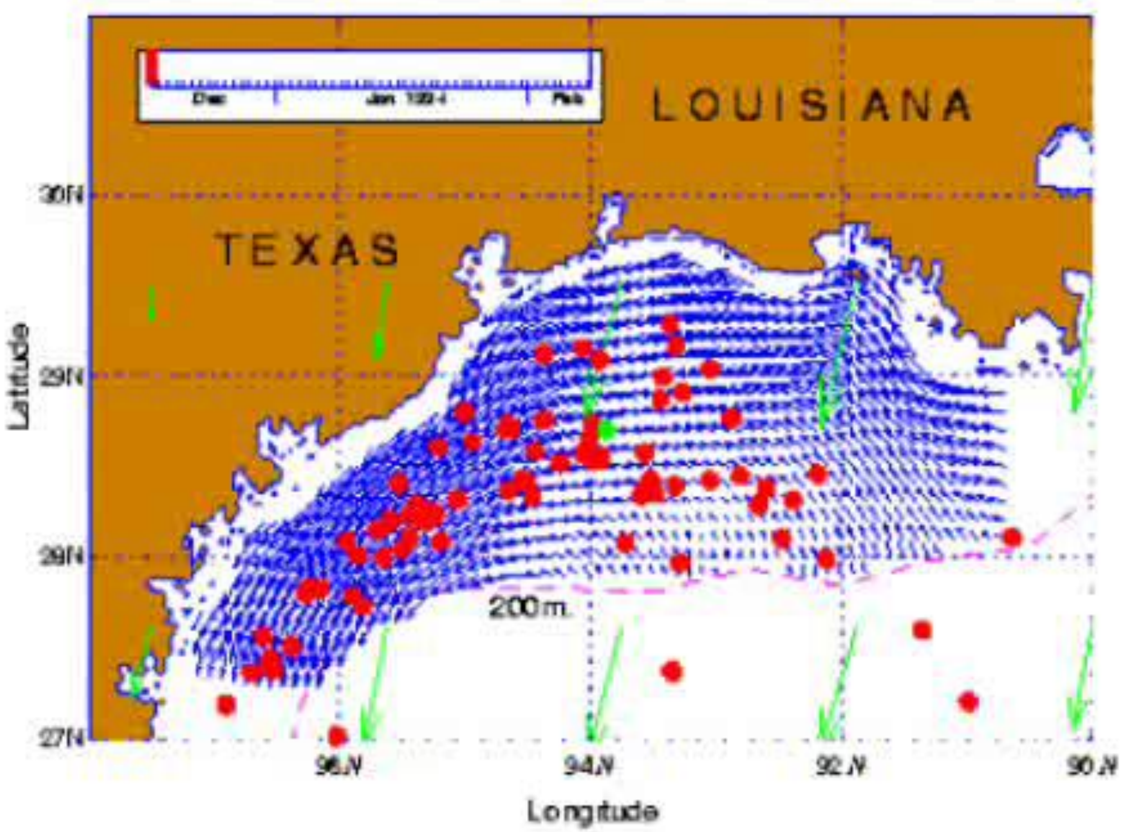

Dec
Jan 1994
Feb
LOUISIANA
TEXAS
200m.
30N
29N
28N
27N
Latitude
96 W
94 W
92 W
90 W
Longitude

LTCS current reversal detected from the reconstructed velocity data

December 30, 1993

January 3, 1994

January 6, 1994

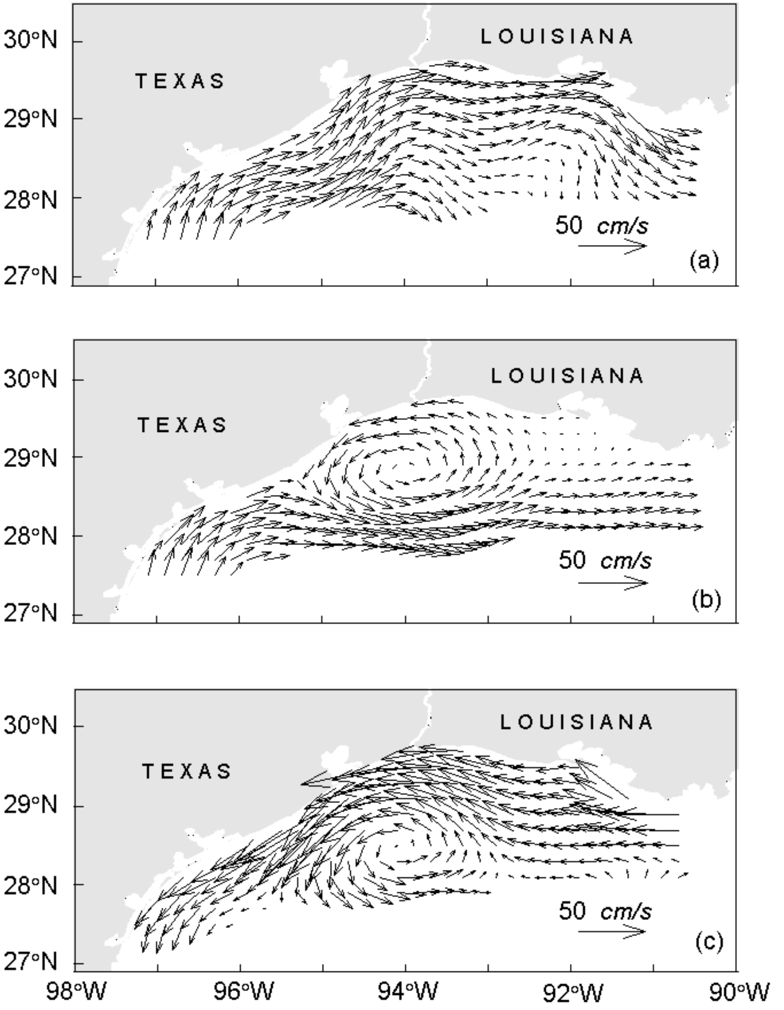

EOF Analysis of the Reconstructed Velocity Filed

EOF	Variance (%)		
	01/21/93-05/21/93	12/19/93-04/17/94	10/05/94-11/29/94
1	80.2	77.1	74.4
2	10.1	9.5	9.3
3	3.9	5.6	6.9
4	1.4	3.3	4.6
5	1.1	1.4	2.3
6	0.7	1.1	0.8

Mean and First EOF Mode

$$\tilde{\mathbf{u}}(x, y, t) = \overline{\mathbf{u}}(x, y) + A_1(t)\mathbf{u}_1(x, y),$$

Mean Circulation

1. First Period (01/21-05/21/93)

2. Second Period 12/19/93-04/17/94)

3. Third Period (10/05-11/29/94)

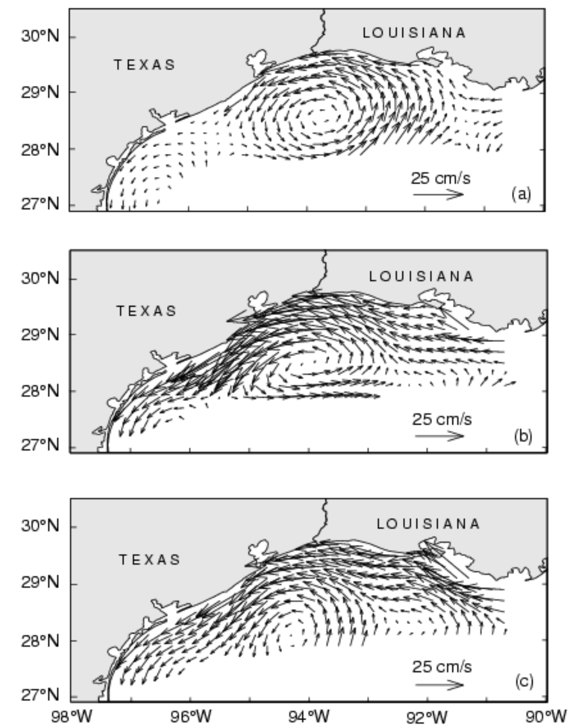

EOF1

1. First Period
(01/21-05/21/93)

2. Second Period
12/19/93-04/17/94)

3. Third Period
(10/05-11/29/94)

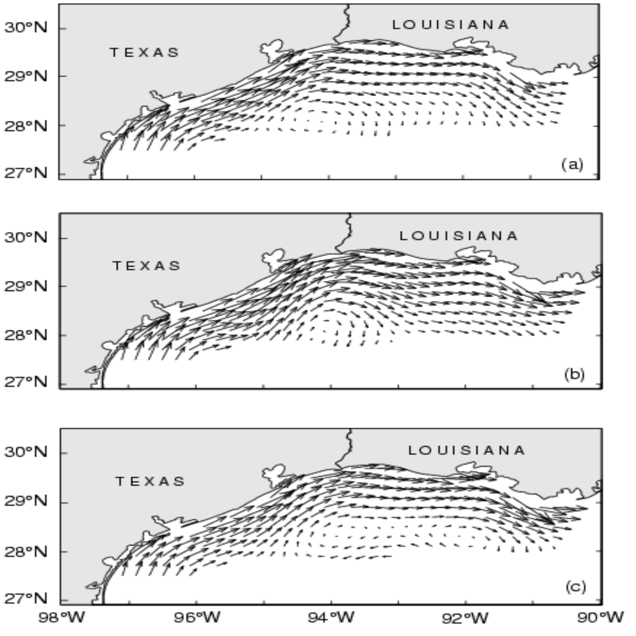

- Calculated $A_1(t)$

Using Current Meter

Mooring (solid)

and SCULP-1

Drifters (dashed)

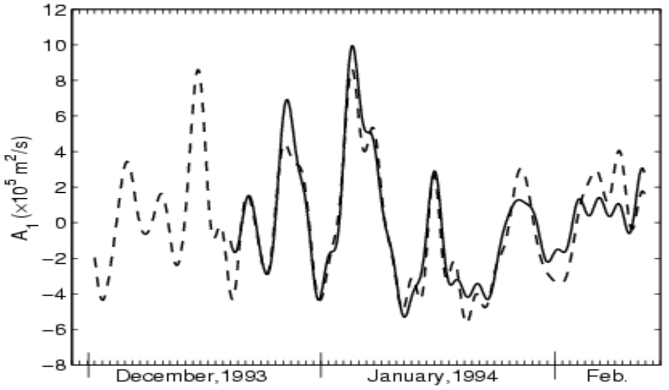

- 8 total reversals observed

$$\eta = A_1^2 / \sum_{n=2}^{6} A_n^2$$

- U_{als} ~ alongshore wind

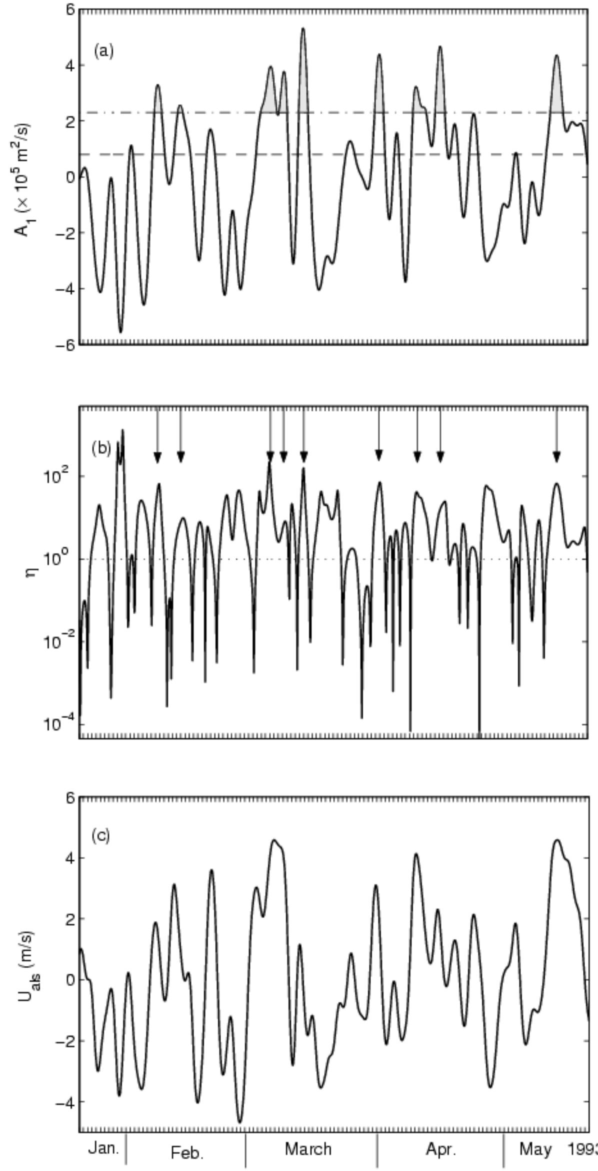

Results

- Alongshore wind forcing is the major factor causing the synoptic current reversal.

- Other factors, such as the Mississippi-Atchafalaya River discharge and offshore eddies of Loop Current origin, may affect the reversal threshold, but can not cause the synoptic current reversal.

(c) Monterey Bay Surface Circulation (CODAR)

CODAR

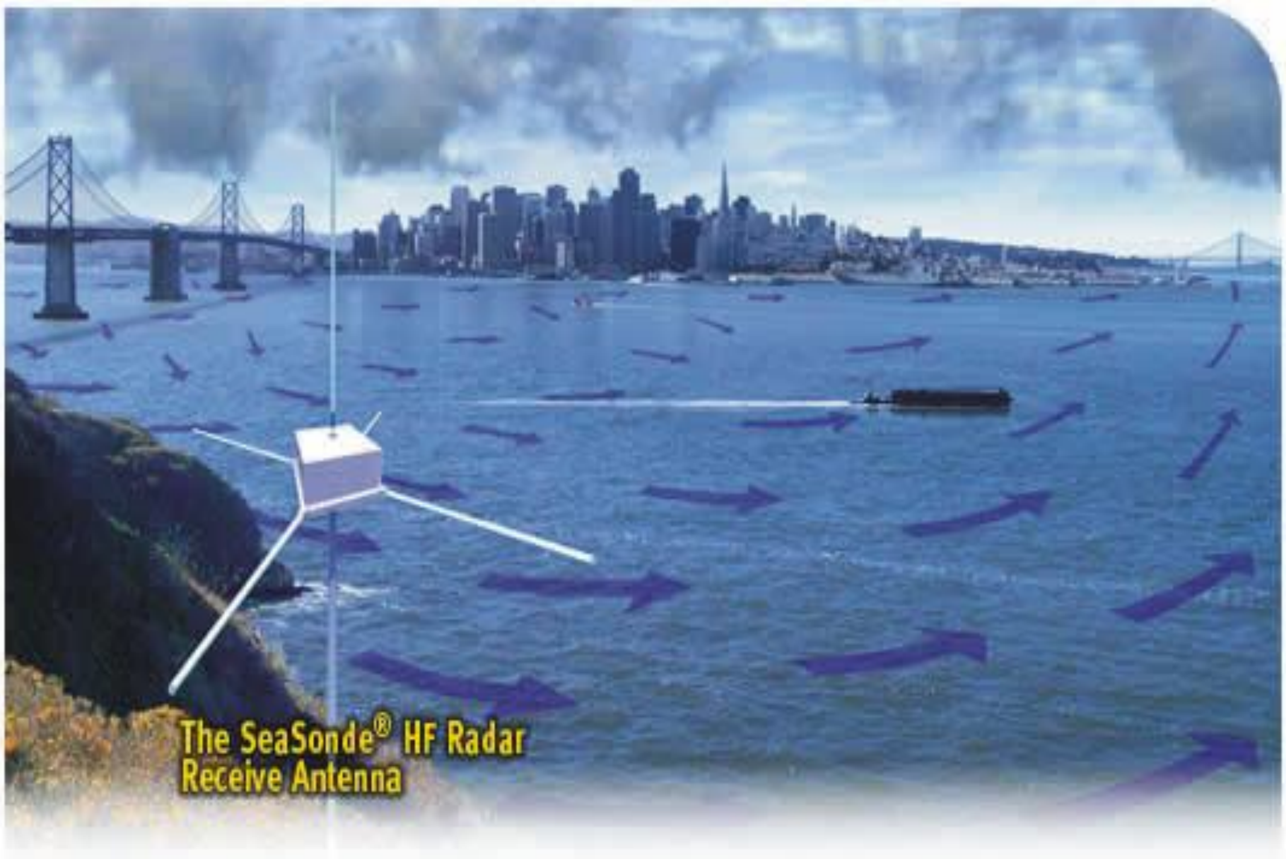

Monterey Bay

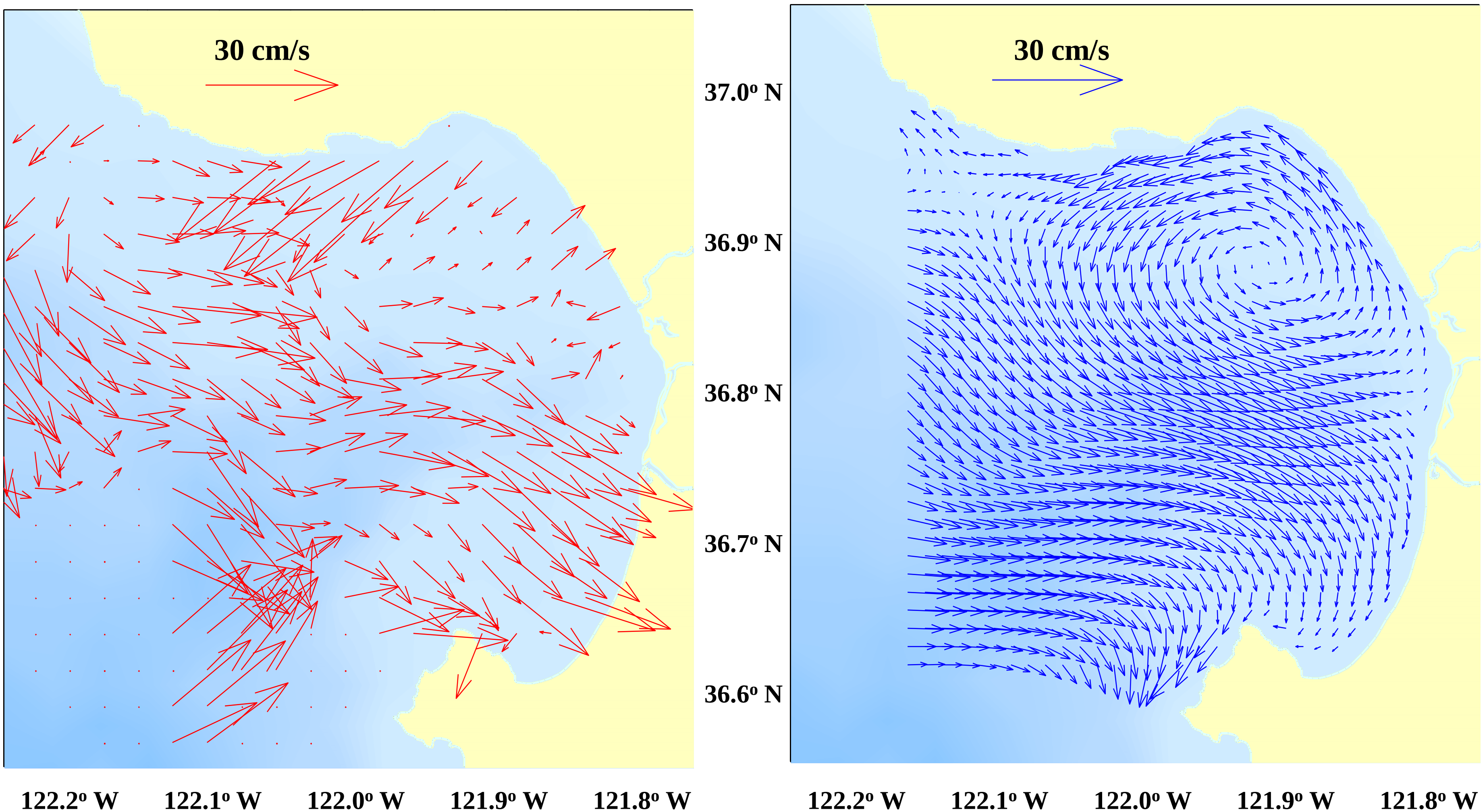

Place for comments: left - radar derived currents for 17:00 UT December 1, 1999

right – reconstructed velocity field.

Preliminary Comparison of OSD and OI Mean (1990-2009)

Visual comparison of the Optimal Spectral Decomposition (OSD)-derived SST (left) to the NOAA Optimally Interpolated (OI) SST (right)

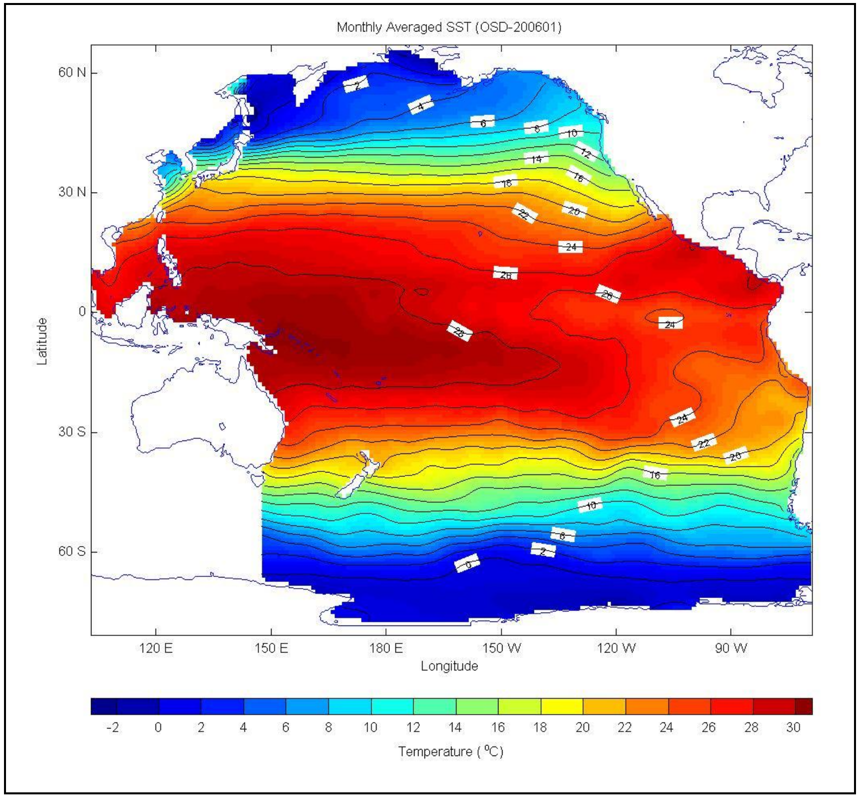

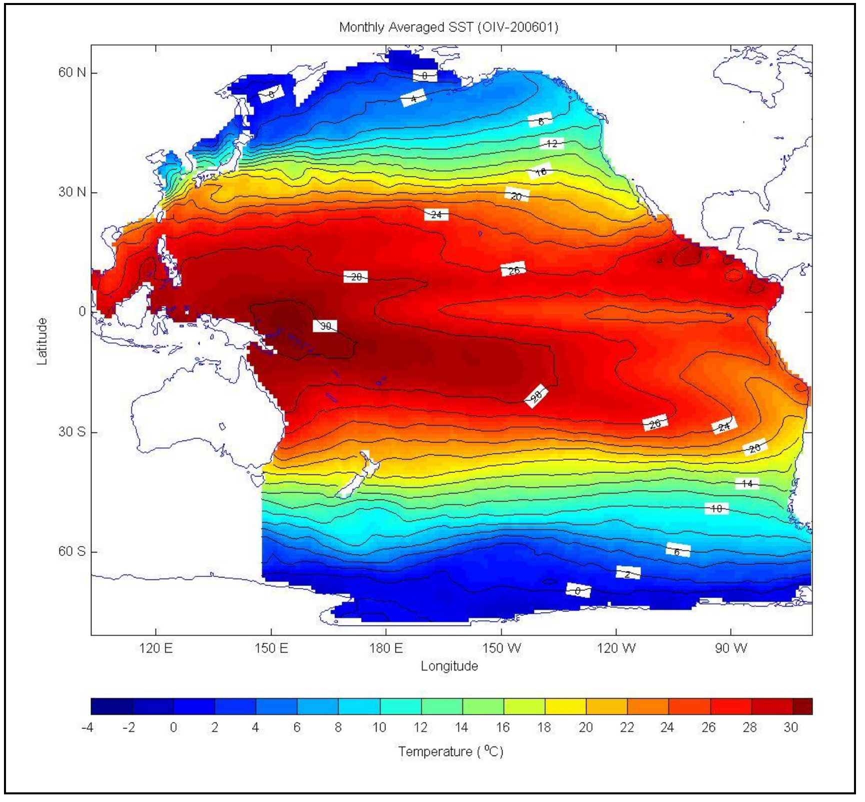

(d) Temporal and spatial variability of Pacific Ocean 1990-2009

Monthly Temperature (10 m) in the Pacific Ocean since 1990 (analyzed from GTSPP)

Monthly Temperature (100 m) in the Pacific Ocean since 1990 (analyzed from GTSPP)

Monthly Temperature (500 m) in the Pacific Ocean since 1990 (analyzed from GTSPP)

Monthly Temperature (1000 m) in the Pacific Ocean since 1990

Conclusions

- OSD is a useful tool for processing real-time velocity data with short duration and limited-area sampling especially the GTSPP/Argo data.
- OSD has wide application in ocean data assimilation.

What is next?

It is an urgent need to establish monthly varying (T, S, u, v) gridded dataset from GTSPP and Argo trajectory data →

Oceanographic and Climate Studies

Steps for GTSPP Data Analysis

- (1) Change the current data format “one file for one profile” into new data format “one file for profiles in a month from January 1990 for individual ocean basin (Atlantic, Pacific, Indian oceans).

- (2) Reconstruct the profile data with the same month and year into grid points using the Optimal Spectral Decomposition (OSD) method.

4D Global Velocity Data

Reference + Geostrophic

(T, S)